CHEMISTRY OF MATERIALS

Article

pubs.acs.org/cm

# Synthesis of Monoclinic and Tetragonal Chalcocite Nanoparticles by Iron-Induced Stabilization

Tony Machani, Daniel P. Rossi, Brandon J. Golden, Evan C. Jones, Mona Lotfipour, and Katherine E. Plass*

Department of Chemistry, Franklin & Marshall College, Lancaster, Pennsylvania 17604, United States

Supporting Information

**ABSTRACT:** Infrared absorbing monoclinic and tetragonal chalcocite nanoparticles were synthesized. These metastable copper sulfide phases were obtained by addition of varying amounts of iron to the reaction mixtures. Phases were identified by powder X-ray diffraction (PXRD), and the particles were characterized by UV−vis−NIR absorption spectroscopy (UV−vis−NIR), transmission electron microscopy (TEM), and energy dispersive X-ray spectroscopy (EDS). This synthesis affords monoclinic chalcocite, which is difficult to obtain in nanocrystalline form because of its ready transformation to copper-deficient djurleite. Nanoparticles of the little-studied, high-temperature-stable tetragonal chalcocite form were synthesized for the first time. These particles showed improved phase stability compared to monoclinic chalcocite, while maintaining the optical properties that made monoclinic chalcocite intensely investigated as a light absorber in photovoltaics. Together, these syntheses offer two routes toward managing an impediment to utilization of nanocrystalline chalcocite in photovoltaic applications, the transformation to djurleite, and uncover remarkable methods of nanocrystalline phase control.

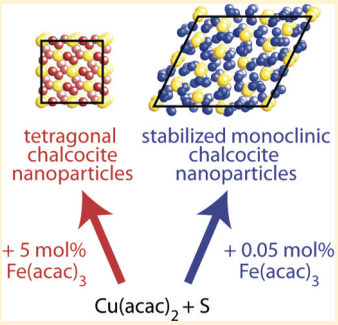


**KEYWORDS:** *copper sulfide, light absorbers, band gap, phase selective, gamma chalcocite, alpha chalcocite, djurleite*

Inexpensive nanocrystalline semiconductor light absorbers have the potential to advance the low-cost, scalable production of photovoltaics and photoelectrochemical cells necessary to meet the projected 30 TW energy demand.[1] This work presents the synthesis of phase-stabilized chalcocite nanoparticles; chalcocite is a particularly promising solar energy conversion material because of its low cost, widespread availability, and potential for generation of ample amounts of electricity (greater than current worldwide consumption).[2] The syntheses of stabilized monoclinic and tetragonal chalcocite particles presented here contribute to the rapidly growing literature reporting earth-abundant semiconductor nanoparticle light absorbers. Such materials, including $Cu_2ZnSnS_4$,[3] SnS,[4] PbO,[5] PbS,[6] and $FeS_2$,[7] have band gaps that enable efficient solar energy conversion[8] as well as readily available constituent elements.

Nanocrystals of chalcocite and the copper-deficient djurleite phase have been extensively studied in past years because of their photovoltaic or plasmonic properties,[9] using several synthetic techniques.[9e,10] Chalcocite transforms into djurleite spontaneously. This phase-instability impeded development of monoclinic-$Cu_2S$:CdS thin film cell photovoltaics.[11] Djurleite formation can reduce photovoltaic efficiency by up to 60% because of shifts in band gap and decrease in the minority carrier diffusion length.[11b] The resultant partially filled bands give rise to plasmonic absorption.[9d,e] Transformation to djurleite is exacerbated in nanoparticles, making it difficult to reliably obtain pure nanoscale monoclinic chalcocite by solution methods.[9e,10h] Even when monoclinic chalcocite nanoparticles are obtained, they rapidly transform to djurleite.[10h] Previous syntheses of nanoscale monoclinic chalcocite depend upon the presence of excess Cu[9d,12] to shift the equilibrium back toward monoclinic chalcocite.[10h,13]

Given the importance of phase-control to copper sulfide-based photovoltaics, we have devised means of stabilizing two different forms of chalcocite nanoparticles with respect to transformation to djurleite by addition of iron complexes to the reaction mixture (Scheme 1). A dependable monoclinic chalcocite nanocrystal synthesis was developed where the conversion to djurleite was impeded by blocking diffusion of copper ions. This is a direct improvement upon synthesis in the absence of iron, where djurelite is obtained in approximately 30% of trials.[10h] Synthesis of tetragonal chalcocite nanoparticles was demonstrated for the first time by addition of yet more iron to the reaction. Tetragonal chalcocite is a high-temperature polymorph of monoclinic and hexagonal chalcocite, which has been little studied.[12e,14] This is also the first time tetragonal chalcocite has been synthesized other than by temperature-induced transformation of monoclinic or hexagonal chalcocite crystals. Addition of Fe(III)$(acac)_3$ to a 2:1 molar ratio of Cu(II)$(acac)_2$:S in oleylamine allows phase-selective synthesis of monoclinic chalcocite, tetragonal chalcocite, and roxbyite, depending upon the amount of Fe added. A typical synthesis involved Cu(II)$(acac)_2$ (2.0 mmol), Fe(III)$(acac)_3$ (between

**Received:** July 30, 2011
**Revised:** November 21, 2011
**Published:** November 23, 2011

**Scheme 1. Effects of the Presence of Iron on the Resultant Nanocrystalline Copper Sulfide Phase[a]**

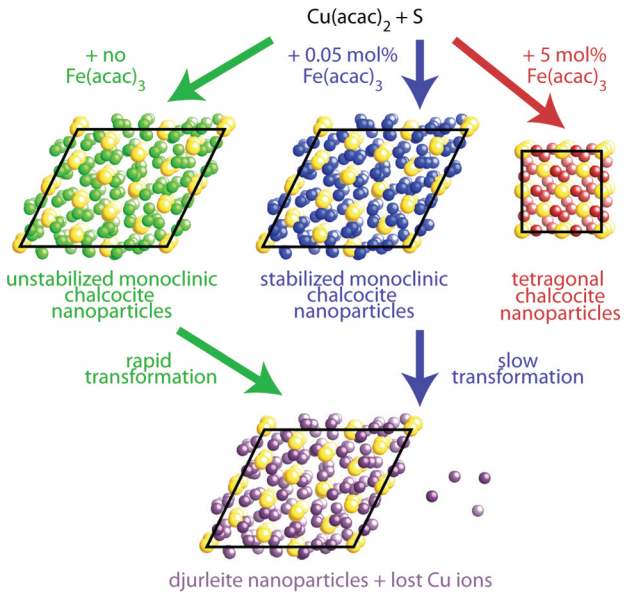


[a]Addition of Fe(III)(acac)$_3$ during the synthetic reaction can alter the solid state structure of the obtained copper sulfide phase or influence the rate at which the obtained particles lose Cu ions to transform to the copper-deficient djurleite phase. The Cu ions are color-coded according to phase.

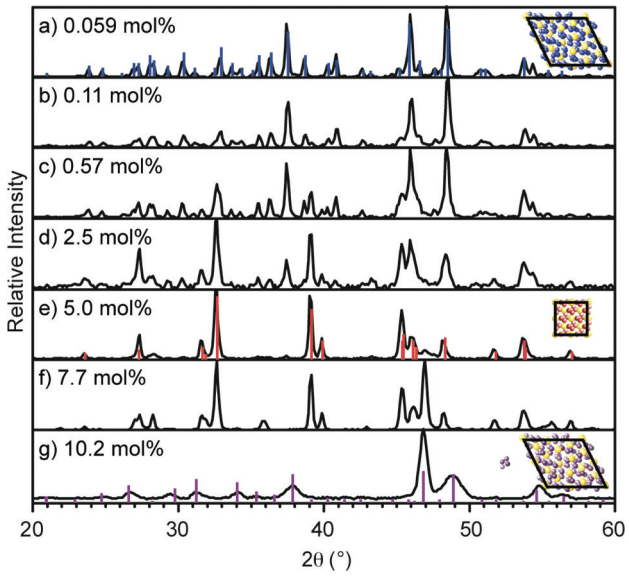


**Figure 1.** PXRD patterns of copper sulfide nanoparticles obtained by addition of various concentrations of Fe(III)(acac)$_3$. Mole ratios are with respect to 0.10 mmol/mL Cu(II)(acac)$_2$. Overlaid are the ICDD patterns for monoclinic chalcocite ([00-023-0961] in blue), tetragonal chalcocite ([01-072-1071] in red), and roxbyite ([00-023-0958] in purple).

0.10 and 0.01 mmol), and elemental S (1.0 mmol) heated in oleylamine to 260 °C (see Supporting Information for more details). Monoclinic and tetragonal chalcocite nanoparticle formation was confirmed by identifying these phases using powder X-ray diffraction (PXRD). Energy dispersive X-ray spectroscopy (EDS) confirmed the chemical composition. Nanoparticle size and morphology was characterized by transmission electron microscopy (TEM). UV−vis−NIR absorption spectroscopy was used to compare the optical properties of monoclinic and tetragonal chalcocite nanoparticles. In an attempt to elucidate the role of Fe in inducing tetragonal chalcocite formation, a series of experiments were undertaken wherein the identity of the added metal complex was varied.

Addition of small amounts of iron to the copper and sulfur-containing reaction mixture allows phase-selective synthesis of monoclinic chalcocite, as shown by the PXRD data in Figure 1a,b. Upon addition of Fe(III)(acac)$_3$ in a molar ratio of 0.00059 Fe:Cu (or 0.059 mol % Fe(III)(acac)$_3$) a diffraction pattern that matches ICDD database pattern [00-023-0961] for monoclinic chalcocite was obtained (Figure 1a). Addition of 0.11 mol % Fe(III)(acac)$_3$ also produces pure monoclinic chalcocite (Figure 1b). Differentiating monoclinic chalcocite and djurleite by PXRD is nontrivial;[9e,10h] however, Figures 1a and b clearly show the peaks at 30.30, 32.84, 38.70, and 40.77° 2$\theta$ and the three-pronged shape of the peak at 46°2$\theta$ that distinguish monoclinic chalcocite (see Supporting Information, Figure S1). Note that without addition of an iron complex, the same synthetic conditions may form monoclinic chalcocite, but often significant amounts of djurleite are also observed.[10h] Addition of this small amount of Fe stabilizes monoclinic chalcocite with respect to the otherwise more preferred nonstoichiometric djurleite phase.[10h,11a,13] In large surface area nanoparticles, transformation of monoclinic chalcocite to copper-deficient djurleite is accelerated by the ready diffusion of copper ions from the bulk.[10h] Incorporation of a small concentration of Fe ions, too low to be detectable via EDS or XPS (see Supporting Information, Figure S2), likely blocks the pathways by which copper ions would diffuse from the monoclinic chalcocite crystal. Monoclinic chalcocite nanoparticles synthesized without iron under these conditions transformed completely to djurleite after a few days under ambient conditions[10h] (surface oxidation speeds transformation). Particles obtained using iron resisted complete transformation to djurleite for at least 35 days (Figure 2 and Supporting Information, Figure S3). In comparison, the presence of a large excess of copper prevented degradation for two weeks.[10h] Djurleite formation is not completely blocked by the presence of iron, but it is slowed significantly. Furthermore, a new method for stabilization of monoclinic chalcocite nanoparticles has been demonstrated. In thin films, doping with $Zn^{2+}$ or $Cd^{2+}$ has been reported to stabilize the monoclinic chalcocite structure, though replacement of Fe(III)(acac)$_2$ with Zn or Cd precursors was not effective at producing monoclinic chalcocite nanoparticles.[10h] This might be indicative that $Fe^{2+}$ more effectively blocks the $Cu^{+}$ diffusion than either $Zn^{2+}$ or $Cd^{2+}$. Alternatively, $Zn^{2+}$ and $Cd^{2+}$ may not be as readily incorporated into the copper sulfide matrix in this solution phase synthesis because of incompatible reaction rates or side-reactions. This suggests that other ions could be employed to stabilize monoclinic chalcocite if appropriate reaction conditions were discovered.

While monoclinic chalcocite nanoparticle formation was induced at low Fe concentrations, tetragonal chalcocite is formed at higher concentrations. When 0.57 mol % Fe(III)(acac)$_3$ is added (Figure 1c) a mixture of monoclinic and tetragonal chalcocite is obtained. When the amount of Fe(III)(acac)$_3$ is increased to 2.5% (Figure 1d), the ratio of tetragonal to monoclinic chalcocite increases. At 5.0 mol % the PXRD pattern shows only peaks due to tetragonal chalcocite


dx.doi.org/10.1021/cm2022196 | Chem. Mater. 2011, 23, 5491–5495

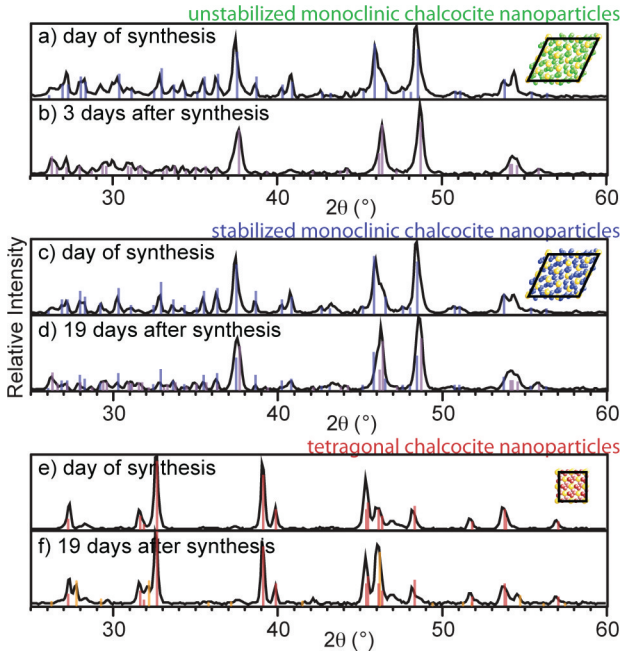


**Figure 2.** PXRD patterns of nanoparticles of monoclinic chalcocite grown in the absence (a,b) and presence of iron complex (c,d) and tetragonal chalcocite (e,f). Patterns are shown as collected on the day of synthesis (a,c,e) and after 3 days (b) or 19 days (d, f). Overlaid are the ICDD patterns for monoclinic chalcocite ([00-023-0961] in blue), tetragonal chalcocite ([01-072-1071] in red), djurleite ([00-023-0959] in purple), and digenite ([00-047-1748], in orange).

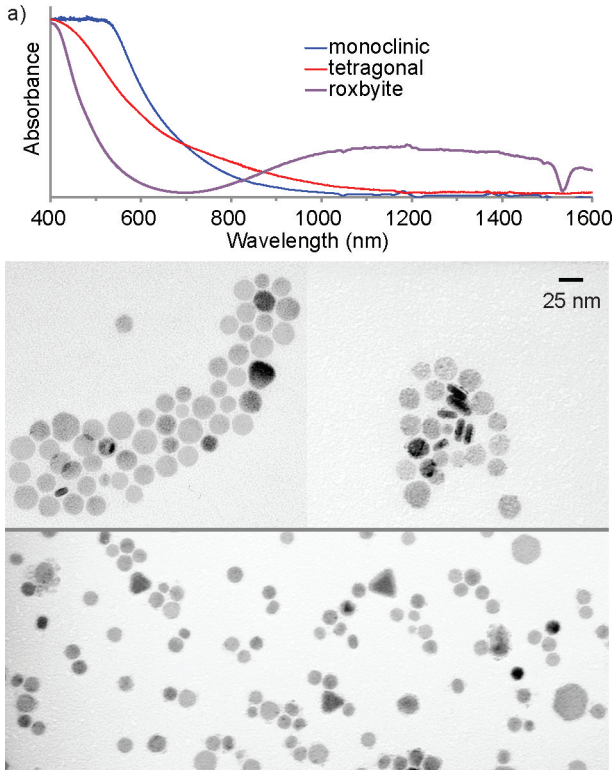


**Figure 3.** (a) UV−vis−NIR absorption spectra of monoclinic (blue) and tetragonal (red) chalcocite nanoparticles obtained with addition of 5 mol % Fe. Both spectra show absorbance onsets of 1100−1200 nm. In comparison, roxbyite nanoparticles (purple) obtained with 10 mol % Fe, show a higher energy onset (700 nm) and significant sub-bandgap absorption. TEM images of (b,c) monoclinic and (c) tetragonal chalcocite at 150,000× magnification.

(Figure 1e). The obtained PXRD pattern matches ICDD database pattern [01-072-1071] for tetragonal chalcocite. All 14 distinct peaks in the database pattern match the obtained pattern. Because of the cubic structure of tetragonal chalcocite, there is no obfuscation of the assignment with other copper sulfide forms (Supporting Information, Figure S4). Thus, pure tetragonal chalcocite as assessed by PXRD is obtained when Fe(III) is added in a narrow concentration range around 5.0 mol %. Less Fe results in a mixture with monoclinic chalcocite and more produces first a mixture of tetragonal chalcocite and nonstoichiometric copper sulfide roxbyite (Figure 1f), then pure roxbyite (Figure 1g) at 10.2 mol %. It is perhaps surprising that this large amount of Fe does not either produce a copper iron sulfide species, like bornite ($Cu_5FeS_4$), or a mixture of iron and copper sulfide species, though both possibilities are ruled out by PXRD (Supporting Information, Figures S5, S6). EDS measurements of Cu and S molar ratios reveal some replacement of Cu by Fe ions and an excess of sulfur. The observed stoichiometry was $Cu_{1.4\pm0.3}Fe_{0.05+0.02}S$, indicating that the ratio of Cu:Fe is slightly less than in solution, and that the phase is highly copper-deficient. XPS shows that while Cu is primarily in the $Cu^+$ state, some +2 is present (Supporting Information, Figure S2). Stabilization of tetragonal chalcocite by iron is reminiscent of the behavior of another copper sulfide phase, digenite ($Cu_{1.80}S$). This phase is known to be stabilized in the bulk by incorporation of Fe into the lattice, and is only found naturally when iron is present.[15]

One notable feature of the obtained tetragonal chalcocite particles is that the observed band gap is very similar to that of monoclinic chalcocite, but that it exhibits improved phase stability. The band gap of tetragonal chalcocite nanoparticles was measured by UV−vis−NIR absorption spectroscopy to be slightly lower than that of monoclinic chalcocite (Figure 3a), as is apparent from the lower energy absorption onset. Onset absorbances around 1200 and 1000 nm are observed for tetragonal and monoclinic particles, respectively. This infrared absorbing behavior makes these interesting materials not only for photovoltaics, but also for NIR photodetectors.[16] No sub-band gap absorbance is observed, which suggests that no amorphous djurleite or digenite are present.[9e] A spectrum of roxbyite nanoparticles obtained with larger amount of Fe is shown in Figure 3a. It illustrates plasmon absorption. Plots of $\sqrt{(\alpha)}$ and $(\alpha)^2$ versus the photon energy shed some light on the nature and magnitude of the band gap of tetragonal chalcocite particles. Because the $\sqrt{(\alpha)}$ values better fit to a straight line than $(\alpha)^2$, we can deduce that the band gap is indirect.[17] From the *x*-intercept of this best fit line, the band gap was measured to be 1.06 ± 0.05 eV. This measurement of a band gap lower than either $\alpha$- or $\beta$-chalcocite is in disagreement with calculations.[13] While no experimental data on tetragonal chalcocite could be found in the literature, the band gaps for both monoclinic and tetragonal chalcocite fall within the range of reported chalcocite band gaps.[18] This shift may represent the optical band gap of pure tetragonal chalcocite or doping with Fe may be altering the light absorption. This cannot be addressed without an independent means of obtaining tetragonal chalcocite nanoparticles. The stability of the obtained tetragonal chalcocite particles was observed over time (Supporting Information, Figure S8). PXRD patterns of the obtained tetragonal chalcocite particles remain little-changed over more than two weeks of storage under ambient


dx.doi.org/10.1021/cm2022196 | *Chem. Mater.* 2011, 23, 5491−5495

conditions that promote degradation to nonstoichiometric phases. In the bulk, tetragonal chalcocite is metastable at atmospheric pressure, and slowly transforms to monoclinic chalcocite.[14a] This perhaps explains why tetragonal chalcocite has not previously been investigated as a photovoltaic material and its electron transport properties have not been studied. Here, instead, very slow transformation to a cubic non-stoichiometric digenite phase is observed. In comparison to monoclinic chalcocite, which requires little movement of the sulfur framework to transform to djurleite,[19] tetragonal chalcocite[20] has a much greater energetic barrier to overcome to transform to djurleite. The additional stability of tetragonal chalcocite may be based solely on the incompatibility of the crystal structures, rather than the presence of iron. This resistance to transformation may make tetragonal chalcocite particles an alternative to monoclinic chalcocite nanoparticle light absorbers in photovoltaic devices in which djurleite is detrimental to performance.

To distinguish the role that Fe(III) plays in controlling the obtained copper sulfide phase, a series of related transition metal species were substituted in the reaction. First, Fe(III)-$(acac)_3$ and Fe(II)$(acac)_2$ both induced tetragonal chalcocite formation at the same concentrations (Figure 4a,b). Given the

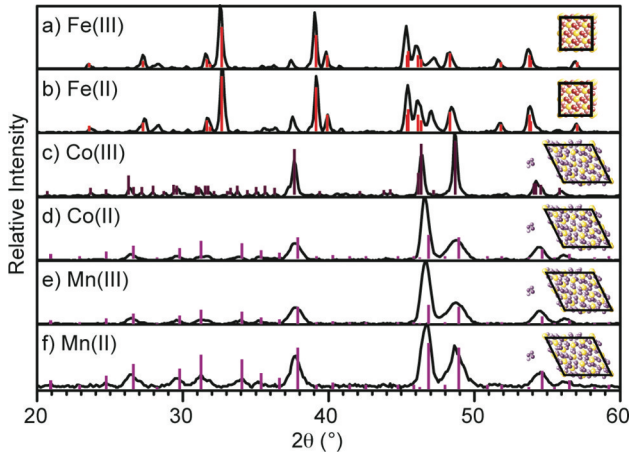


**Figure 4.** PXRD patterns of copper sulfide nanoparticles obtained by addition of 5.0 mol % of various metal acetylacetonates to the Cu(II)$(acac)_2$ and S-containing reaction mixture. Only addition of Fe species (a,b) induces formation of tetragonal chalcocite. Co (c,d) and Mn (e,f) induce formation of djurleite or roxbyite.

highly reducing oleylamine environment and high temperatures, it is likely that Fe(III) species are transformed to Fe(II), and that Fe(II) is the species that interacts with and alters chalcocite crystallization. High temperature polymorphs of zirconia are stabilized by doping with yttria and with a wide range of other dopants with the same valence.[21] To test whether tetragonal chalcocite might display similar generality, the following experiment was carried out. The 3+ transition metal species Cr(III)$(acac)_3$, Mn(III)$(acac)_3$, and Co(III)-$(acac)_3$ and the 2+ species Mn(II)$(acac)_2$ and Co(II)$(acac)_2$ were separately introduced into the reaction mixture ratios at 0.1:2.0 metal:Cu molar ratios. None of these five species induced tetragonal chalcocite formation, instead resulting in djurleite or roxbyite formation (Figure 4c–f). One potential explanation could be the seeding of crystals by tetragonal FeS nuclei, which have unit cell constants very similar to those of tetragonal chalcocite. All other manganese, cobalt, and chromium sulfide structures reported in the Inorganic Crystal Structure Database have significantly larger unit cells or hexagonal symmetries incompatible with the tetragonal chalcocite structure (Supporting Information, Table S1 and Figure S9). Alternative mechanisms, like the oxygen-vacancy induced stabilization of high temperature zirconia phases caused by the presence of yttria and other dopants, cannot be ruled out.[21]

Transmission electron microscopy (Figures 3b,c,d) shows that both monoclinic (Figure 3b,c) and tetragonal (Figure 3d) chalcocite nanoparticles are generally shapeless, with hexagonal particles in both reactions. In Figure 3c platelets seem to be present, viewed from the side. Tetragonal nanoparticles also form some triangular tetragonal chalcocite particles, suggesting that shape control may be possible. Monoclinic chalcocite particles are more monodisperse, with average diameters of 20.4 ± 3.0 nm while the tetragonal particles have a similar size (average diameters of 16.1 ± 6.6 nm) with greater variation in size and shape.

Phase-control in chalcocite nanoparticles, one impediment to the use of these earth-abundant particles for low-cost photovoltaic applications, has been addressed by the discovery that incorporation of iron stabilizes the obtained solid-state phase. Either monoclinic or tetragonal chalcocite nanoparticles can be selected under these conditions, and both phases are stabilized with respect to the tendency to lose Cu atoms and transform to djurleite when compared to nanoparticles obtained in the absence of iron complex. The stabilization of monoclinic chalcocite by doping suggests avenues for improving properties of nanoparticles or rods synthesized by thermolysis from solution or by cation exchange. Tetragonal chalcocite nanoparticles are novel materials that combine an improved stability over monoclinic chalcocite with very similar optical properties. Uncovering a detailed mechanism for stabilization of this high temperature phase may uncover means of phase-engineering other metal chalcogenide particle phases.

## ■ ASSOCIATED CONTENT

### Supporting Information

Experimental details, a discussion of how to distinguish djurleite and $\alpha$-chalcocite by PXRD, XPS of tetragonal and iron-stabilized monoclinic chalcocite nanoparticles, PXRD patterns of monoclinic chalcocite particles monitored over time stored under ambient conditions, comparison of PXRD patterns between tetragonal nanoparticles with database, PXRD patterns of tetragonal chalcocite particles monitored over time stored under ambient conditions, unit cell parameters for possible seed crystals. This material is available free of charge via the Internet at http://pubs.acs.org.

## ■ AUTHOR INFORMATION

### Corresponding Author

*E-mail: kplass@fandm.edu.

## ■ ACKNOWLEDGMENTS

The authors thank Franklin & Marshall College for start-up funds, for student grants, and for student support via the Hackman Summer Scholars Program, as well as the Henry and Camille Dreyfus Foundation for a New Faculty Startup Award and Research Corporation for a Cottrell College Science Award. Electron microscopy measurements were made possible

by Prof. Robert Jinks and through the Penn Regional Nanotechnology Facility, Materials Research Facilities Network of the MRSEC Program of the National Science Foundation under award #DMR05-20020, and the assistance of Dr. Douglas Yates and Dr. Lolita Rotkina.

## REFERENCES

(1) (a) Gur, I.; Fromer, N. A.; Geier, M. L.; Alivisatos, A. P. *Science* **2005**, *310*, 462−465. (b) Lewis, N. S.; Nocera, D. G. *Proc. Natl. Acad. Sci. U.S.A.* **2006**, *103*, 15729−15735. (c) Nozik, A. J. *Nano Lett.* **2010**, *10*, 2735−2741.

(2) Wadia, C.; Alivisatos, A. P.; Kammen, D. M. *Environ. Sci. Technol.* **2009**, *43*, 2072−2077.

(3) (a) Guo, Q. J.; Hillhouse, H. W.; Agrawal, R. *J. Am. Chem. Soc.* **2009**, *131*, 11672−11673. (b) Riha, S. C.; Parkinson, B. A.; Prieto, A. L. *J. Am. Chem. Soc.* **2009**, *131*, 12054−12055. (c) Steinhagen, C.; Panthani, M. G.; Akhavan, V.; Goodfellow, B.; Koo, B.; Korgel, B. A. *J. Am. Chem. Soc.* **2009**, *131*, 12554−12555.

(4) Liu, H. T.; Liu, Y.; Wang, Z.; He, P. *Nanotechnology* **2010**, *21*, 105707.

(5) Cattley, C. A.; Stavrinadis, A.; Beal, R.; Moghal, J.; Cook, A. G.; Grant, P. S.; Smith, J. M.; Assender, H.; Watt, A. A. R. *Chem. Commun.* **2010**, *46*, 2802−2804.

(6) Watt, A. A. R.; Blake, D.; Warner, J. H.; Thomsen, E. A.; Tavenner, E. L.; Rubinsztein-Dunlop, H.; Meredith, P. *J. Phys. D: Appl. Phys.* **2005**, *38*, 2006−2012.

(7) (a) Puthussery, J.; Seefeld, S.; Berry, N.; Gibbs, M.; Law, M. *J. Am. Chem. Soc.* **2011**, *133*, 716−719. (b) Wadia, C.; Wu, Y.; Gul, S.; Volkman, S. K.; Guo, J. H.; Alivisatos, A. P. *Chem. Mater.* **2009**, *21*, 2568−2570.

(8) Shockley, W.; Queisser, H. J. *J. Appl. Phys.* **1961**, *32*, 510−519.

(9) (a) Wu, Y.; Wadia, C.; Ma, W. L.; Sadtler, B.; Alivisatos, A. P. *Nano Lett.* **2008**, *8*, 2551−2555. (b) Lee, H.; Yoon, S. W.; Kim, E. J.; Park, J. *Nano Lett.* **2007**, *7*, 778−784. (c) Page, M.; Niitsoo, O.; Itzhaik, Y.; Cahen, D.; Hodes, G. *Energy Environ. Sci.* **2009**, *2*, 220−223. (d) Alivisatos, A. P.; Luther, J. M.; Jain, P. K.; Ewers, T. *Nat. Mater.* **2011**, *10*, 361−366. (e) Zhao, Y. X.; Pan, H. C.; Lou, Y. B.; Qiu, X. F.; Zhu, J. J.; Burda, C. *J. Am. Chem. Soc.* **2009**, *131*, 4253−4261.

(10) (a) Zhuang, Z. B.; Peng, Q.; Zhang, B.; Li, Y. D. *J. Am. Chem. Soc.* **2008**, *130*, 10482−10483. (b) Zhang, H. T.; Wu, G.; Chen, X. H. *Langmuir* **2005**, *21*, 4281−4282. (c) Zhang, H.; Zhang, Y. Q.; Yu, J. X.; Yang, D. R. *J. Phys. Chem. C* **2008**, *112*, 13390−13394. (d) Sigman, M. B.; Ghezelbash, A.; Hanrath, T.; Saunders, A. E.; Lee, F.; Korgel, B. A. *J. Am. Chem. Soc.* **2003**, *125*, 16050−16057. (e) Lu, Q. Y.; Gao, F.; Zhao, D. Y. *Nano Lett.* **2002**, *2*, 725−728. (f) Lim, W. P.; Wong, C. T.; Ang, S. L.; Low, H. Y.; Chin, W. S. *Chem. Mater.* **2006**, *18*, 6170−6177. (g) Lim, W. P.; Low, H. Y.; Chin, W. S. *Cryst. Growth Des.* **2007**, *7*, 2429−2435. (h) Lotfipour, M.; Machani, T.; Rossi, D. P.; Plass, K. E. *Chem. Mater.* **2011**, *23*, 3032−3038.

(11) (a) Putnis, A. *Philos. Mag.* **1976**, *34*, 1083−1086. (b) Chopra, K. L.; Das, S. R. *Thin Film Solar Cells*; Plenum Press: New York, 1983.

(12) (a) Lai, C. X.; Wu, Q. B.; Chen, J.; Wen, L. S.; Ren, S. *Nanotechnology* **2010**, *21*, 215602. (b) Gorai, S.; Ganguli, D.; Chaudhuri, S. *Mater. Chem. Phys.* **2004**, *88*, 383−387. (c) Wang, S. H.; Guo, L.; Wen, X. G.; Yang, S. H.; Zhao, J.; Liu, J.; Wu, Z. H. *Mater. Chem. Phys.* **2002**, *75*, 32−38. (d) Wang, S. H.; Yang, S. H. *Chem. Phys. Lett.* **2000**, *322*, 567−571. (e) Wang, S. H.; Yang, S. H. *Adv. Mater. Opt. Electron.* **2000**, *10*, 39−45. (f) Zhao, S. Z.; Han, G. Y.; Li, M. Y. *Mater. Chem. Phys.* **2010**, *120*, 431−437.

(13) Lukashev, P.; Lambrecht, W. R. L.; Kotani, T.; van Schilfgaarde, M. *Phys. Rev. B* **2007**, *76*, 195202.

(14) (a) Skinner, B. J. *Econ. Geol.* **1970**, *65*, 724−730. (b) Serebrya, Nr *Geochem. Internat. USSR* **1966**, *3*, 687−&.

(15) Morimoto, N.; Gyobu, A. *Am. Mineral.* **1971**, *56*, 1889−1909.

(16) Konstantatos, G.; Levina, L.; Tang, J.; Sargent, E. H. *Nano Lett.* **2008**, *8*, 4002−4006.

(17) Pankove, J. I. *Optical Processes in Semiconductors*; Dover Publications: New York, 1971.

(18) Rodriguez-Lazcano, Y.; Martinez, H.; Calixto-Rodriguez, M.; Rodriguez, A. N. *Thin Solid Films* **2009**, *517*, 5951−5955.

(19) Evans, H. T. *Science* **1979**, *203*, 356−358.

(20) Janosi, A. *Acta Crystallogr.* **1964**, *17*, 311−312.

(21) (a) Li, P.; Chen, I. W.; Pennerhahn, J. E. *J. Am. Ceram. Soc.* **1994**, *77*, 118−128. (b) Li, P.; Chen, I. W. *J. Am. Ceram. Soc.* **1994**, *77*, 1281−1288.